[CANCER RESEARCH 64, 2357–2364, April 1, 2004]

Identification of a Novel Mammary-Restricted Cytochrome P450, CYP4Z1, with Overexpression in Breast Carcinoma

Michael A. Rieger,[1] Reinhard Ebner,[3] David R. Bell,[4] Andrea Kiessling,[1] Jacques Rohayem,[2] Marc Schmitz,[1] Achim Temme,[1] E. Peter Rieber,[1] and Bernd Weigle[1]

Institutes of [1]Immunology and [2]Virology, Medical Faculty Carl Gustav Carus, Technical University of Dresden, Dresden, Germany; [3]Avalon Pharmaceuticals, Germantown, Maryland; and [4]Molecular Toxicology, University of Nottingham, Nottingham, United Kingdom

ABSTRACT

By screening a transcriptome database for expressed sequence tags that are specifically expressed in mammary gland and breast carcinoma, we identified a new human cytochrome P450 (CYP), termed CYP4Z1. The cDNA was cloned from the breast carcinoma line SK-BR-3 and codes for a protein of 505 amino acids. Moreover, a transcribed pseudogene *CYP4Z2P* that codes for a truncated CYP protein (340 amino acids) with 96% identity to CYP4Z1 was found in SK-BR-3. *CYP4Z1* and *CYP4Z2P* genes consisting of 12 exons are localized in head-to-head orientation on chromosome 1p33. Tissue-specific expression was investigated using real-time reverse transcription PCR with normalized cDNA from 18 different human tissues. *CYP4Z1* mRNA was preferentially detected in breast carcinoma tissue and mammary gland, whereas only marginal expression was found in all other tested tissues. Investigation of cDNA pairs from tumor/normal tissues obtained from 241 patients, including 50 breast carcinomas, confirmed the breast-restricted expression and showed a clear overexpression in 52% of breast cancer samples. The expression profile of *CYP4Z2P* was similar to that of *CYP4Z1* with preference in breast carcinoma and mammary gland but a lower expression level in general. Immunoblot analyses with a specific antiserum for CYP4Z1 clearly demonstrated protein expression in mammary gland and breast carcinoma tissue specimens as well as in CYP4Z1-transduced cell lines. Confocal laser-scanning microscopy of MCF-7 cells transfected with a fluorescent fusion protein CYP4Z1-enhanced green fluorescent protein and a subcellular fractionation showed localization to the endoplasmic reticulum as an integral membrane protein concordant for microsomal CYP enzymes.

INTRODUCTION

The probability of developing breast cancer during a life span is one woman in eight in the United States today. Although mortality rates declined by 1.4% per year during 1989–1995 and by 3.2% afterward, breast cancer is still the second leading cause of cancer death in women (estimated 39,800 deaths in 2003 in the United States; Ref. 1). The identification of a large variety of tumor-associated antigens, which are specifically expressed in cancer tissue, is an essential need for promising immunotherapy of minimal residual disease and for early diagnosis of primary cancer. Unfortunately, the number of potent antigens is still very limited for breast cancer (2).

In this study, the search for new highly restricted breast cancer antigens in a commercial transcriptome database revealed the sequence of an expressed sequence tag (EST) that showed homology to sequences of the cytochrome P450 (CYP) superfamily. In humans, CYPs are involved in the synthesis of cholesterol, steroids, and other lipids and, furthermore, in drug metabolism and in degradation of xenobiotics (3, 4). By elongation of the EST, we identified the cDNA of a new member of CYP subfamily 4Z, designated CYP4Z1. In general, the CYP4 family consisting of six subfamilies (A, B, F, V, X, and Z) in humans has the unique ability to catalyze the thermodynamically disfavored ω-hydroxylation of fatty acids and is mainly implicated in metabolism of arachidonic acid, fatty acids, prostaglandins, and other eicosanoids (5–7).

Many CYPs are expressed extrahepatically and might play an important role in target tissue metabolic activation of xenobiotic compounds (8, 9). Moreover, the presence of CYP enzymes in various cancer tissues emphasizes the possibility of this class of enzymes to either contribute to carcinogenicity of xenobiotics (10) or to influence the impact of anticancer agents positively or negatively (11–14). In organs of the respiratory and gastrointestinal tract with initial exposure to xenobiotics, expression of CYP enzymes 1A1, 1B1, and 3A, among others, was reported (15–19), and extensive studies exist that reveal their high contribution in generating genotoxic products. The smoke-inducible CYP1A1 converts polycyclic aromatic hydrocarbons (*e.g.,* 7–12-dimethylbenz[α]anthracene; Ref. 20), whereas CYP3A enzymes are able to activate aflatoxins (21), heterocyclic amines (22), and nitrosamines (23). CYP1B1, an extrahepatically expressed CYP with significant overexpression in many different tumor types (24), is capable of activating the following variety of putative human carcinogens: polycyclic aromatic hydrocarbons; aromatic and heterocyclic amines (25); and aflatoxin B1 (26). In human mammary gland and uterus, the expression of CYP1B1 has been implicated in 4-hydroxylation of estradiol, a process that may affect estrogen-initiated carcinogenesis by the production of depurinating genotoxic byproducts (27, 28). Additionally, for one member of the CYP4 family, CYP4B1, which is mainly expressed extrahepatically in lung and bladder (29), its possible involvement in carcinogenesis by activating 4-ipomeanol (30), 3,3′-dichlorobenzidine, and 2-naphthylamine (31) was reported.

Therefore, the main aim of this study was to investigate the tissue distribution of this novel CYP by quantitative real-time reverse transcription (RT)-PCR and, particularly, to evaluate the overexpression in breast cancer found by microarray analysis in view of its potential use as a breast cancer-related antigen.

MATERIALS AND METHODS

Chemicals. The breast adenocarcinoma cell lines SK-BR-3 (HTB-30) and MCF-7 (HTB-22) as well as human embryonic kidney cells 293T were acquired from American Type Culture Collection (Manassas, VA). EBV-transformed lymphoblastoid B cells (B-LCL) were a gift from A. F. Kirkin (Danish Cancer Society, Copenhagen, Denmark). Restriction enzymes, Rapid DNA Ligation kit, and DNase I were purchased from MBI Fermentas (St. Leon-Rot, Germany). Titanium *Taq*DNA polymerase (BD Clontech, Heidelberg, Germany) was routinely used for PCR. All other chemicals of molecular biology grade were obtained either from Sigma Chemical Company (Taufkirchen, Germany) or Merck AG (Darmstadt, Germany).

Cell Culture. SK-BR-3 and MCF-7 cells were maintained in monolayer culture, B-LCL in suspension, in a humidified 5% CO_2 atmosphere using RPMI 1640 supplemented with *N*-acetyl-L-alanyl-L-glutamine (2 mM), nonessential amino acids (1×), sodium pyruvate (1 mM) and FCS (10%; Biochrom KG, Berlin, Germany). 293T cells were cultivated in DMEM with 10% FCS.

Received 4/1/03; revised 12/31/03; accepted 1/26/04.

Grant support: Pinguin-Foundation, Düsseldorf, Germany; MeDDrive, Medical Faculty Carl Gustav Carus, TU Dresden, Germany; InnoRegio, BMBF 03i4019, Bonn, Germany; and The Wellcome Trust (054778), United Kingdom.

The costs of publication of this article were defrayed in part by the payment of page charges. This article must therefore be hereby marked *advertisement* in accordance with 18 U.S.C. Section 1734 solely to indicate this fact.

Requests for reprints: Bernd Weigle, Institute of Immunology, Technical University Dresden, Fetscherstrasse 74, 01307 Dresden, Germany. Phone: 0049-351-4586524; Fax: 0049-351-4586316; E-mail: weigle@rcs.urz.tu-dresden.de.

All adherent cells were passaged using trypsin/EDTA (Invitrogen, Karlsruhe, Germany) at 80–90% confluence.

Bioinformatics. EST clustering and homology searches were performed using Heidelberg Unix Sequence Analysis Resources.[5] UniGene clusters and chromosomal maps were investigated with biocomputing services of the National Center for Biotechnology Information.[6]

RNA Isolation and First Strand cDNA Synthesis. Total RNA from cell lines was isolated using the RNeasy Mini kit (Qiagen, Hilden, Germany). One μg DNA-free RNA was reverse transcribed with oligodeoxythymidylic acid primer into first strand cDNA using the Advantage RT-for-PCR kit (BD Clontech) following the manufacturer's instructions.

Cloning of Full-Length *CYP4Z* cDNAs. Either first strand cDNA from SK-BR-3 or pooled mammary gland marathon ready cDNA (BD Clontech) was used for PCR with the following oligonucleotide primers: 4Z_N, 5′-AGAATGGAGCCCTCCTGGCTTCAG-3′ and 4Z_C, 5′-ATTTCCCTTCG-CAGTGGAAGTCAGC-3′. PCR was run on a PTC-200 thermal cycler (MJ Research, Waltham, MA) as follows: 95°C for 30 s, 65°C for 30 s, and 68°C for 2.5 min (36 cycles). PCR products were cloned either into pCR2.1, pCRII-TOPO, or pCR4-TOPO vectors (Invitrogen) and analyzed by sequencing.

Real-Time RT-PCR. Sixteen human normal tissue cDNAs [Multiple Tissue cDNA (MTC) panel I and II; BD Clontech] are provided as first strand cDNA pooled from 2 to 45 healthy donors and normalized against four housekeeping genes (G3PDH, β-actin, α-tubulin, and phospholipase A2). cDNA of human breast cancer tissue and of corresponding normal tissue from five individuals was purchased as a cDNA panel (BD Clontech) normalized against two housekeeping genes (β-actin, 23-kDa highly basic protein). cDNAs of normal breast specimens or cancerous breast tissue were pooled and normalized to MTC panel I and II with β-actin-specific (actin_N1 5′-GCCGTCTTCCCCTCCATCGTG-3′ and actin_C1 5′-GGAGCCACACG-CAGCTCATTGTAGA-3′) and hypoxanthine phosphoribosyltransferase-specific (hypoxanthine phosphoribosyltransferase_N1 5′-CCCTGGCGTCGTG-ATTAGTGATGAT-3′ and hypoxanthine phosphoribosyltransferase_C1 5′-TGCTTTGATGTAATCCAGCAGGTCAGC-3′) real-time PCR.

Quantitative RT-PCR was performed with the LightCycler instrument (Roche, Mannheim, Germany) and Fast Start DNA Master SYBR Green I kit (Roche). The following primers were used for specific amplification: Z1_N, 5′-CTTTCCAGATGGACGCTCCTTACCT-3′ and Z1_C, 5′-GGCAAAAT-GCTGCCCAATGCAGTTC-3′ for CYP4Z1; Z1_N and Z2_C, 5′-CCAG-CAAGGAAATTAGAATTACTTAATCC-3′ for CYP4Z2P. Two μl of each cDNA was used in 20 μl of reaction volume (4 mM $MgCl_2$, 0.5 μM of each oligonucleotide primer, and 10% SYBR Green I Mix). The annealing temperature was 66°C. Forty (CYP4Z1) or 50 cycles (CYP4Z2P) were performed. The specificity of each PCR product was routinely checked by melting curve analysis and by sequencing. The expression level in the normalized tissue samples was calculated by subtracting the crossing point (ct), determined by Fit point analysis, of distinct tissue samples from the ct of the liver cDNA sample (for CYP4Z1 PCR) or from the ct of the prostate cDNA sample (for CYP4Z2P PCR) and by raising the PCR efficiency to the power of the ct difference. Therefore, the expression level of a certain cDNA is given as x-fold expression in the tested tissue to the expression in liver (liver = 1) or prostate (prostate = 1). The expression level of each transcript was determined in three individual experiments, and mean values and SE are illustrated.

Cancer Profiling Array. A 310 bp fragment of the 3′ region of *CYP4Z1* cDNA was labeled with [^{32}P]dCTP (3000 Ci/mmol; Amersham Biosciences, Freiburg, Germany) using the Mega Prime DNA Labeling System (Amersham Biosciences) and hybridized to a commercially available Cancer Profiling Array (BD Clontech) representing 241 tumor/normal cDNA pairs of 12 different tissue types (all normalized) according to the manufacturer's instructions. The array was exposed to a phosphor-imaging screen. Signals were densitometrically analyzed using the Phoretix advanced 1D v4.01 software (Phoretix, Newcastle, United Kingdom).

Retroviral Vectors and Transduction of Cells. To express CYP4Z1 in heterologous cells, the full-length cDNA of *CYP4Z1* was cloned into the *Eco*RI site of the Moloney murine leukemia virus-derived vector pcz-CFG5.1-IRES2-enhanced green fluorescent protein (EGFP) resulting in the vector pcz-CFG5.1-CYP4Z1-IRES2-EGFP.

For construction of pcz-CFG5.1-IRES2-EGFP, the IRES2-EGFP fragment of pIRES2EGFP (BD Clontech) was ligated into the *Bam*HI and *Hpa*I sites of pcz-CFG5.1-MCS (32) creating pcz-CFG5.1-IRES2-EGFP.

Recombinant retroviral particles were generated by using the three vector-packaging system according to the procedures described by Soneoka *et al.* (33). Briefly, 293T cells were transiently cotransfected with an expression construct for gag-pol (pHIT60), the MoMuLV-based retroviral vectors, and the vesicular stomatitis virus G-protein (pMD.G2; provided by D. Trono, University of Geneva, Switzerland). Viral supernatants were harvested 48 and 72 h after transfection, pooled, and filtered (0.45-μm pore size filter). Polybrene was added to a final concentration of 8 μg/ml, and supernatants were used immediately or stored at −80°C. MCF-7 and B-LCL cells were infected with retroviral particles containing either CYP4Z1-IRES2-EGFP or IRES2-EGFP. The transduction efficiency was 83–85% for MCF-7 cells and 73–77% for B-LCL.

Immunoblot Analysis of CYP4Z1. Polyclonal antiserum specific for CYP4Z1 from New Zealand White rabbits was generated against the peptide CPDHSRPPQPVRQVVLKSK (position 477–494 of CYP4Z1) coupled to keyhole limpet hemocyanine via the reactive side chain on the NH_2-terminal Cys residue. To analyze CYP4Z1 expression in MCF-7 and B-LCL cells transduced either with CYP4Z1-IRES2-EGFP or IRES2-EGFP, cells were resuspended and boiled in 1× Laemmli buffer (34) for 8 min. Cell equivalents (3×10^5) per sample were analyzed by SDS-PAGE (34) and immunoblotting using anti-CYP4Z1 serum (1:1000) and horseradish peroxidase-linked goat antirabbit IgG (1:10,000; Chemicon, Hofheim, Germany) in combination with enhanced chemiluminescent detection (ECL plus; Amersham Biosciences). Whole-cell protein lysates of mammary gland tissue and breast carcinoma tissue were purchased from Biocat (Heidelberg, Germany). Fifty μg of tissue lysate was subjected to SDS-PAGE and immunoblotting.

Confocal Laser-Scanning Analyses. The coding sequence of *CYP4Z1* cDNA was amplified by PCR using forward primer 5′-GCTAGCATGGAGC-CCTCCTGGCTTCAGGAA-3′ and reverse primer 5′-TCTAGACCG-CAAACTTTTTTTGCAAACAC-3′, which replaces the stop codon with the codon for glycine and cloned into pCRII-TOPO vector. After *Nhe*I/*Xba*I digestion of this vector, the insert was ligated into the *Nhe*I site of the mammalian expression vector pEGFP-C1 (BD Clontech). The resulting plasmid termed pCYP4Z1-EGFP codes for a fusion protein of CYP4Z1 and EGFP on the COOH-terminus. pmRFP1, which is a derivative of pEGFP-C3 (BD Clontech) and codes for the monomeric red fluorescent protein 1 (mRFP1), was a gift from R. Y. Tsien (35). This vector was used to create the following reporter constructs for specific organelle staining. The vector pmRFP1-endoplasmic reticulum (ER) codes for the human Sec61 β subunit, an ER membrane protein, which is fused to the COOH-terminal of mRFP1 (36). pmRFP1-Mito codes for the native rat aldehyde dehydrogenase mitochondrial presequence (19 amino acids) plus the first 23 amino acid residues from the mature region fused to mRFP1 (37). MCF-7 cells were grown on chamber slides to 90–95% confluence and were transiently cotransfected with 0.5 μg of plasmid DNA of pCYP4Z1-EGFP and either pmRFP1-ER or pmRFP1-Mito using Lipofectamine 2000 (Invitrogen) according to the manufacturer's instructions. After transfection (24–30 h), cells were fixed with 4% paraformaldehyde for 15 min, washed three times with PBS, and analyzed by confocal laser scanning microscopy (NCS-NT; Leica, Wetzlar, Germany) using the filters SP590, DD488/568, RSP580, and LP530/30 or LP590 for detection of EGFP or mRFP1, respectively.

Subcellular Fractionation. Subcellular organelle fractionation of MCF-7 cells transduced with CYP4Z1 was basically performed as described previously (38). All steps were carried out at 4°C. Briefly, CYP4Z1 expressing MCF-7 cells were resuspended in buffer HB [0.5 M sucrose, 10 mM Tris (pH 7.4), 1 mM EDTA and protease inhibitor mixture tablet (Complete Mini, EDTA-free; Roche)] to 4×10^7 cells/ml. Cells were homogenized by passing through a 26-gauge needle for several times and three bursts (50% output level/50% duty cycle) of an ultrasonic disintegrator (Sonifier 250; Branson, Dietzenbach, Germany). After adding an equal volume of 10 mM Tris pH 7.4, 1 mM EDTA, the homogenate was layered onto one-half volume of buffer HB and centrifuged at $1200 \times g$ for 10 min using a swing-out bucket (SW-55T, Beckman L7–65 ultracentrifuge). The supernatant was layered onto one-half volume of buffer HB and centrifuged at $10{,}000 \times g$ for 10 min. To obtain the microsomal-enriched fraction, the resulting supernatant was spun at $100{,}000 \times g$ for 1 h at 4°C. The pellet obtained after each centrifugation step

[5] Heidelberg Unix Sequence Analysis Resources, http://genome.dkfz-heidelberg.de.
[6] National Center for Biotechnology Information, http://www4.ncbi.nlm.nih.gov/.

was carefully resuspended in 300 μl of 0.25 M sucrose, 10 mM Tris (pH 7.4), and 1 mM EDTA. P1 (1,200 × *g*) contains nuclei and cellular debris, P2 (10,000 × *g*) is the mitochondria-enriched fraction and P3 (100,000 × *g*) comprises the microsome-rich fraction. The supernatant after ultracentrifugation (S3) is designated the soluble protein fraction.

Sodium Carbonate Extraction of Extrinsic Proteins from Microsomes. One hundred μg of the microsomal fraction P3 was diluted in ice-cold 1 ml of 0.1 M sodium carbonate and incubated for 30 min on ice followed by centrifugation at 100,000 × *g* for 1.5 h at 4°C. The pellet was resuspended in 20 μl of Laemmli buffer. Proteins of 500 μl supernatant were precipitated by trichloroacetic acid treatment and resuspended in 10 μl of Laemmli buffer. Ten μl of the resuspended pellet and of the precipitated supernatant were subjected to SDS-PAGE and analyzed by immunoblotting with polyclonal anti-CYP4Z1 serum.

Immunoblot Analysis of Subcellular Fractions. Equal volumes of fractions P1, P2, and P3 and the corresponding volume of S3 were subjected to SDS-PAGE and analyzed by immunoblotting. Polyclonal rabbit anti-CYP4Z1 serum was used to detect CYP4Z1 protein. Immunoblot analysis of endogenous mitochondrial HSP60 protein (monoclonal anti-HSP60; Biocarta, Hamburg, Germany) and ER membrane-bound calnexin (monoclonal anticalnexin, BD Biosciences, Heidelberg, Germany) was used as an independent assay of the separation of the subcellular fractions. Horseradish peroxidase-conjugated secondary antibody rabbit antimouse immunglobulins (1:1000; Dako, Hamburg, Germany) were visualized with enhanced chemiluminescence (ECL plus; Amersham Biosciences).

RESULTS

Evidence of a New Breast Cancer Candidate in the Database GeneExpress. The transcriptome database GeneExpress (Gene Logic Inc., Gaithersburg, MD) contains expression profiles of a large number and variety of different human normal and tumor tissues obtained by Affymetrix GeneChip analyses. Our search for new genes, which are specifically expressed in mammary gland and overexpressed in breast cancer, revealed an EST with the GenBank accession number AI668602, represented by the chip element 59570_at that showed sequence similarity with the 3′ region of members of the CYP family. The EST is mainly expressed in mammary gland tissue samples and hardly ever found in other normal female tissues (2%; Fig. 1).

Furthermore, 61% of malignant breast tissues are positive with a median expression more than twice as high as normal breast tissue expression. Even more prominent, in the 25% positive carcinoma samples with the highest expression, a fluorescence signal of at least 1315 units was detected contrasting 414 units for the corresponding value in normal mammary gland. Metastases originating from breast cancer in lymph nodes or in other locations show a similar expression profile as primary tumors (Fig. 1). There are no significant differences between various breast tumor types and different tumor stages (data not shown).

Identification of a New CYP. On the basis of sequence homologies within members of the CYP protein family, the use of bioinformatics enabled us to prolong the EST sequence in its 5′ orientation. Amino acid sequence comparisons of CYP4A11 to human genomic sequence databases by TBlastN2 revealed sequence similarities of at least 50% with genomic regions that are localized close to the 5′ of EST AI668602. These regions of similarity represent putative exons of the newly identified *CYP* gene. The existence of the corresponding mRNA was verified by RT-PCR using oligonucleotide primer pairs that bound in the 3′ untranslated region (EST AI668602) as well as in the predicted exons of the new CYP in cDNA from the breast carcinoma cell line SK-BR-3 and pooled mammary gland cDNA. Having identified the putative start ATG in exon 1 of this new CYP, amplification of full-length cDNA including the coding region revealed the following two different *CYP4Z* transcripts in SK-BR-3: the cDNAs of *CYP4Z1* (GenBank accession number AY262056) and of the pseudogene *CYP4Z2P* (GenBank accession number AY262057). The existence of both new CYP was already expected by the CYP Nomenclature Committee only based on genomic sequences (5).

The nucleotide sequence of *CYP4Z1* cDNA (1907 bp) contains an open reading frame of 1515 bp that codes for a 505 amino acid protein (Fig. 2). Because of sequence homologies and similarity of size to other CYP, the first ATG represents most likely the true translation initiation codon. A polyadenylic acid sequence is preceded by the polyadenylation signal AATAAA at the 3′ untranslated region. The deduced amino acid sequence of CYP4Z1 shows identity >40% to other members of the CYP family 4 and thus belongs to this CYP family after the convention of the CYP Nomenclature Committee (5). The characteristic conserved Cys residue, which serves as the fifth ligand to the heme iron in CYP proteins, is located at amino acid position 452. Conserved P450 sequence motifs and structural characteristics of functional CYP enzymes are met in CYP4Z1.

A single nucleotide change (C to T) in the *CYP4Z2P* cDNA (1436 bp) leads to a nonsense mutation 1020 bp downstream of the translation start. The open reading frame of *CYP4Z2P* cDNA codes for 340 amino acids that are 96% identical to CYP4Z1 protein sequence (Fig. 2).

Genomic Localization of *CYP4Z1* and *CYP4Z2P*. On the basis of genomic analysis by bioinformatics, the genes for CYP4Z1 and CYP4Z2P are both localized on chromosome 1p33 in head-to-head orientation in a distance of 166 kb. The genomic sequence is represented by the genomic contig NT_032977. Both genes *CYP4Z1* and *CYP4Z2P* are composed of 12 exons and 11 introns with highly conserved exon-intron boundaries and span 50.8 kb and 57.3 kb, respectively.

The genes for CYP4A11, CYP4B1, and CYP4×1 are localized

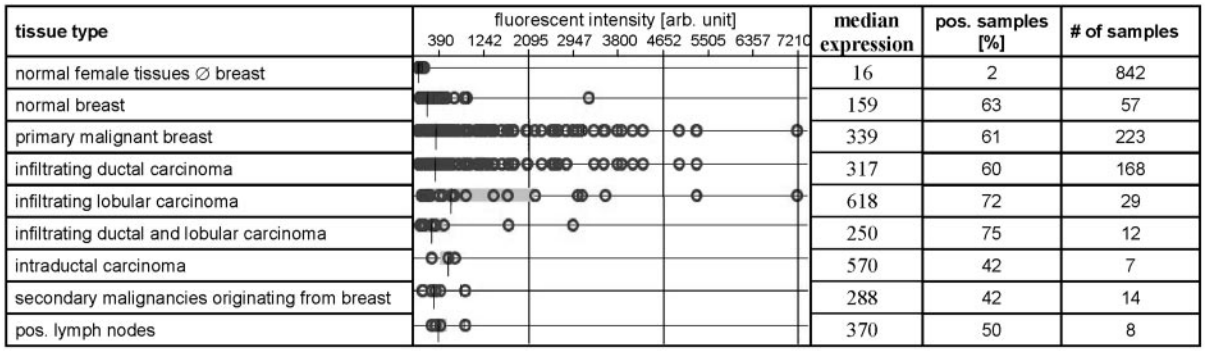

tissue type	median expression	pos. samples [%]	# of samples
normal female tissues ∅ breast	16	2	842
normal breast	159	63	57
primary malignant breast	339	61	223
infiltrating ductal carcinoma	317	60	168
infiltrating lobular carcinoma	618	72	29
infiltrating ductal and lobular carcinoma	250	75	12
intraductal carcinoma	570	42	7
secondary malignancies originating from breast	288	42	14
pos. lymph nodes	370	50	8

Fig. 1. Electronic Northern data of expressed sequence tag AI668602 expression in various tissues obtained from the transcriptome database GeneExpress. Each circle represents a positive sample with its fluorescent intensity. Median expression is illustrated by vertical bars. *Arb. unit*, arbitrary unit; *pos.*, positve.

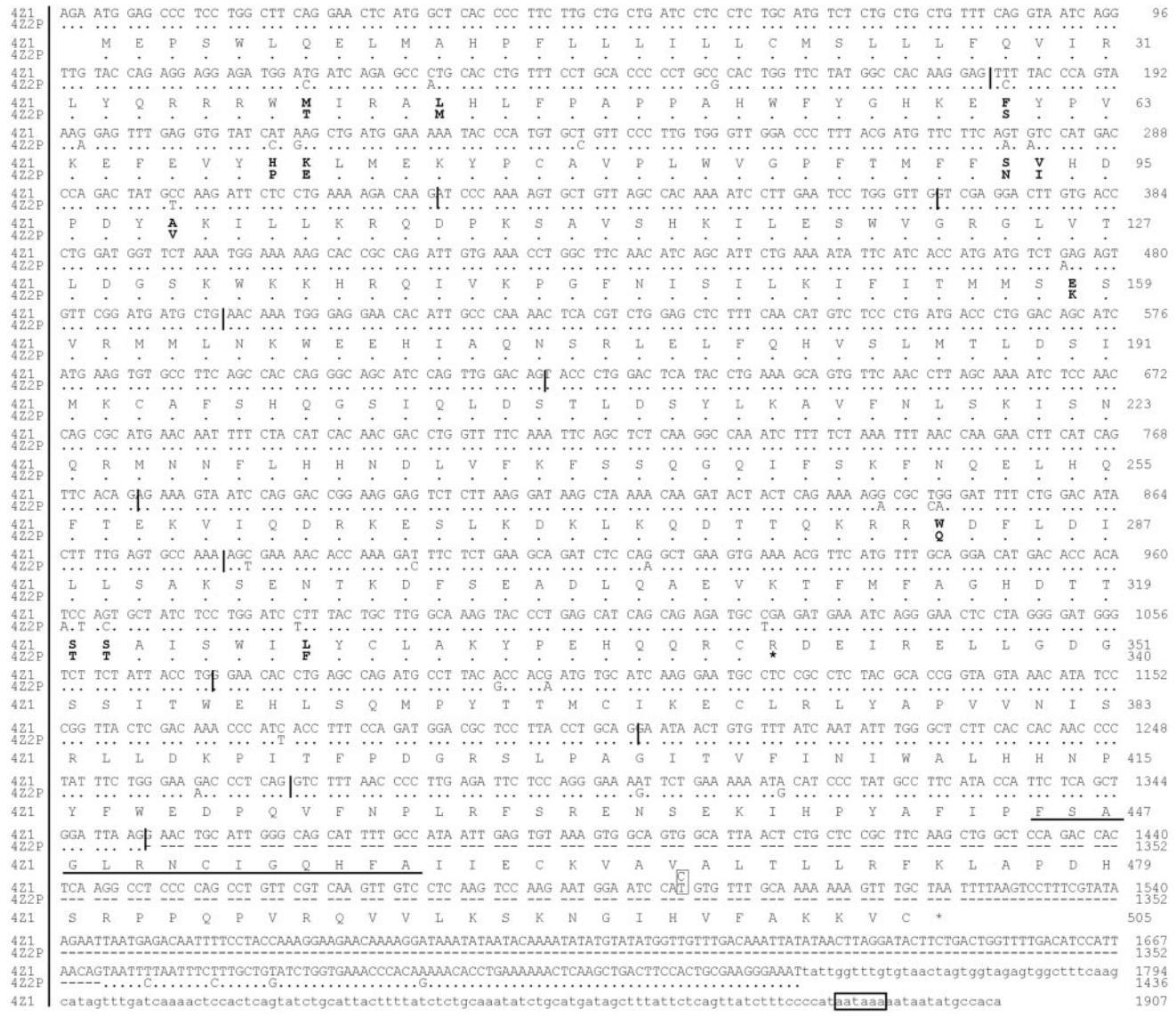

Fig. 2. Nucleotide sequences of *CYP4Z1* and *CYP4Z2P* cDNA and their deduced amino acid sequences. cDNA sequences (in *capitals*) were confirmed by three independent cDNA clones each from SK-BR-3. Silent nucleotide exchange at position 1497 was found in a clone derived from pooled mammary gland cDNA and might represent an allelic variant of *CYP4Z1* (*boxed*). 3′ untranslated region sequence of *CYP4Z1* cDNA was adopted from expressed sequence tag AI668602 (illustrated in *small letters*). Exon borders are signalised by *vertical lines*. The stop codons are illustrated by *asterisks*. The polyadenylation signal is *enframed*. The highly conserved heme-binding site is *underlined*.

closely to the loci of *CYP4Z1* and *CYP4Z2P* on contig NT_032977 representing a cluster of *CYP4* genes.

Mammary Gland-Specific Expression of *CYP4Z1* and CYP4Z2P mRNA. Quantitative real-time RT-PCR was performed to investigate the tissue distribution of *CYP4Z1* and *CYP4Z2P* transcripts in a variety of human tissues. Expression levels were analyzed in normalized pooled cDNA samples from 17 different human normal tissues and from breast cancer tissues as shown in Fig. 3. By far the highest expression of *CYP4Z1* mRNA was observed in breast carcinoma with a 3.6-fold overexpression over normal mammary gland and with a >60-fold higher expression level over any other tested normal female tissue. Only in some samples, there was a marginal amount of transcripts detectable.

CYP4Z2P transcription shows an even more restricted expression pattern than *CYP4Z1* with a 4.8 times higher expression in breast cancer tissue than in normal mammary gland (data not shown). Only in testis, prostate, kidney, and placenta, a few transcripts were found, whereas no *CYP4Z2P* transcription at all was detectable in all other tissues. However, the expression level of *CYP4Z2P* was roughly 20 times lower than that of *CYP4Z1*.

Expression of *CYP4Z1* in Different Tumors and Corresponding Normal Tissues. To obtain information about the *CYP4Z1* expression in various tumors, a cancer profiling array with 241 tumor/normal cDNA pairs from 12 different tissue types was analyzed (Fig. 4*A*). Overall, there was a much higher expression in breast samples (50 pairs) than in other tissues with a variable expression level among breast cancer patients. Seventy-two percent of breast tumor samples and 76% of normal mammary gland tissues were positive. Moreover, a clear overexpression (at least 2-fold, up to 111-fold) in cancerous breast tissue was visible in 52% compared with their corresponding normal tissues (Fig. 4B). A down-regulation in the tumor sample was noticeable in 22% of breast pairs, but the *CYP4Z1* expression was low in these patients in general. The following carcinoma tissues other than breast showed a weak expression of *CYP4Z1*: ovary (4 of 16); lung (3 of 21); thyroid gland (1 of 6); and prostate (2 of 4). There was a marginal signal in five lung and two kidney samples.

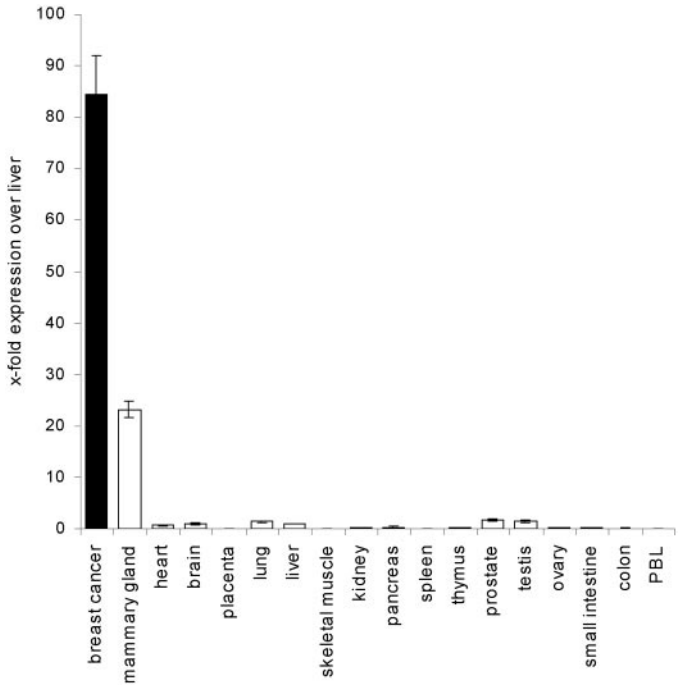

Fig. 3. Tissue expression profile of CYP4Z1 examined with real-time reverse transcription-PCR. *CYP4Z1* expression in 18 human tissues in relation to the expression level in liver. The mean of three individual experiments and the SE is illustrated. *PBL*, peripheral blood lymphocyte.

Detection of CYP4Z1 Protein in Breast Carcinoma Tissue. Expression of CYP4Z1 protein in breast cancer tissue was demonstrated by immunoblotting with a specific antipeptide antiserum for CYP4Z1. Immunoblot analysis revealed a distinct band of approximately 50 kDa representing CYP4Z1 protein in whole-cell lysates of an intraductal carcinoma, an invasive lobular carcinoma, and normal mammary gland tissue as well as in MCF-7 and B-LCL cells transduced with the coding sequence of *CYP4Z1* cDNA (Fig. 5). Lysates of untransduced cells and one invasive ductal carcinoma were negative for CYP4Z1 expression. The protein expression of CYP4Z1 was higher in transduced MCF-7 than in transduced B-LCL cells reflecting the mRNA expression data obtained by quantitative real-time RT-PCR analysis of both cell lines (data not shown).

Subcellular Localization of CYP4Z1 in Human Cells. P450 enzymes in eukaryotes are integral membrane proteins localized either to the inner membrane of mitochondria or to the outer face of the ER. The NH_2-terminal hydrophobic domain serves as a combined signal sequence and transmembrane anchor in ER-bound P450 leading the core enzyme into the cytoplasm. To determine the intracellular localization of CYP4Z1, we transiently transfected MCF-7 cells with a vector coding for EGFP fused to the COOH-terminus of CYP4Z1. Confocal laser-scanning microscopy of CYP4Z1-EGFP showed a typical morphological pattern of ER staining (Fig. 6*A*). CYP4Z1-EGFP protein colocalized perfectly with the cotransfected red fluorescent fusion protein Sec61 β subunit, a component of the protein translocation apparatus of the ER membrane (Fig. 6*A*). No colocalization with the red fluorescent mitochondrial marker protein was visible. The ER localization of the expressed CYP4Z1-EGFP was

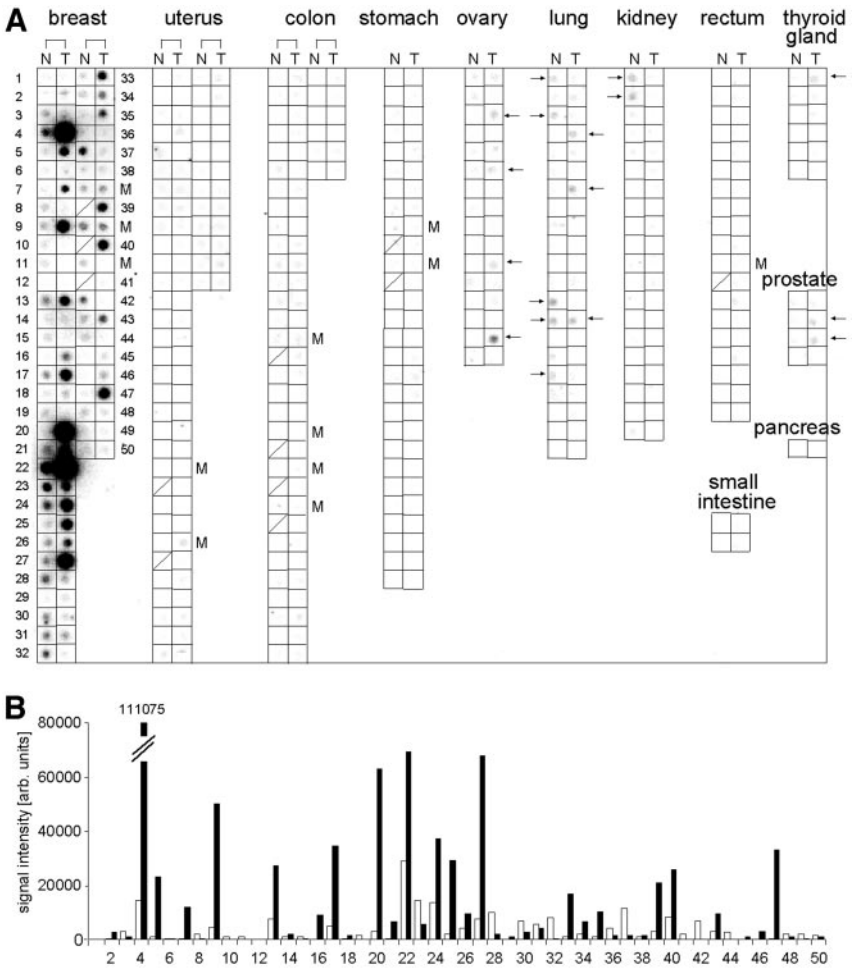

Fig. 4. Expression of *CYP4Z1* in cancerous tissue samples and their corresponding normal tissues. *A*, cancer profiling array hybridized with a ^{32}P-labeled probe. Tissue samples of each individual patient are localized on one row next to each other representing the cancerous tissue sample (*right square*) and its corresponding noncancerous tissue (*left square*). *Arrows* stress weak positive signals. *B*, densitometric determination of signal intensity obtained in (*A*) from breast cancer patients. *Black bars*, cancerous tissue; *white bars*, normal tissue. Patient numbers match in (*A*) and (*B*). *N*, noncancerous tissue samples; *T*, cancerous tissue samples; *M*, tissue sample of corresponding metastasis; *Arb. unit*, arbitrary unit.

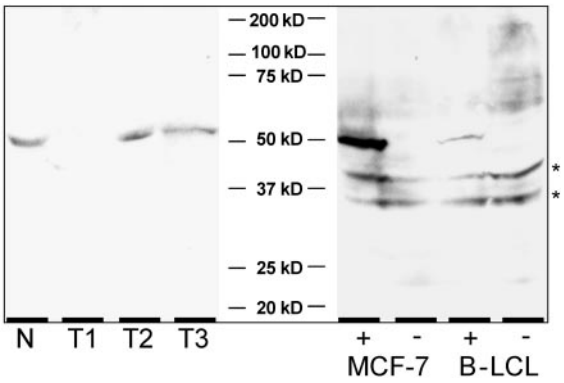

Fig. 5. Immunoblot analysis of CYP4Z1 expression. Whole cell lysates from mammary gland tissue (N), three breast carcinomas (T1-T3; 50 μg/sample), whole cell lysates from MCF-7 cells, and lymphoblastoid B cells (B-LCL; 3×10^5 cell equivalents) were subjected to SDS-PAGE and immunoblotting. MCF-7 and B-LCL cells transduced with retroviral particles containing either CYP4Z1-IRES2-enhanced green fluorescent protein (+) or IRES2-enhanced green fluorescent protein control vector (−). Invasive ductal carcinoma (T1), intraductal carcinoma (T2), invasive lobular carcinoma (T3). *, unspecific staining.

confirmed by subcellular fractionation of MCF-7 cells transduced with *CYP4Z1* cDNA. CYP4Z1 protein was mainly detected in the 100,000 $\times$ *g* pellet (P3) representing the microsomal-enriched fraction after subcellular fractionation (Fig. 6*B*). Only a faint band was detected in the mitochondrial enriched fraction P2. Endogenous mitochondrial HSP60 and ER membrane-bound calnexin were detected mainly in fraction P2 and P3, respectively, confirming the separation of mitochondria and microsomes in the fractionation assay. Extraction with sodium carbonate effectively strips extrinsic proteins off membranes without affecting transmembrane and lipid-anchored proteins. CYP4Z1 was only detected in the insoluble microsomal membrane fraction (*P*) by immunoblot analysis (Fig. 6*C*). This clearly demonstrates its integration into the ER membrane, the native location for microsomal P450 enzymes.

DISCUSSION

We have cloned the cDNAs of two novel *CYP* genes of the 4Z subfamily, *CYP4Z1* and *CYP4Z2P*, and demonstrated preferential expression in human breast carcinoma and mammary gland tissue. Although the existence of *CYP4Z1* has been expected by ESTs in the UniGene entry Hs.176588, the deduced protein sequence of the *CYP4Z1* cDNA we cloned differs from the predicted amino acid sequence by genomic database research, mainly attributable to differences in intron-exon boundaries and possible sequencing errors in genomic contigs. Microsomal P450 enzymes are bound to the ER membrane via an NH_2-terminal transmembrane domain. Cellular localization studies of fluorescent CYP4Z1-EGFP fusion protein by microscopy and subcellular fractionation clearly showed its localization as an integral membrane protein of the ER. The natural distribution to the ER and the presence of P450-essential conserved domains of CYP4Z1 (39) indicate its affiliation as a functional P450 enzyme, but additional analyses proving its functionality have to be performed.

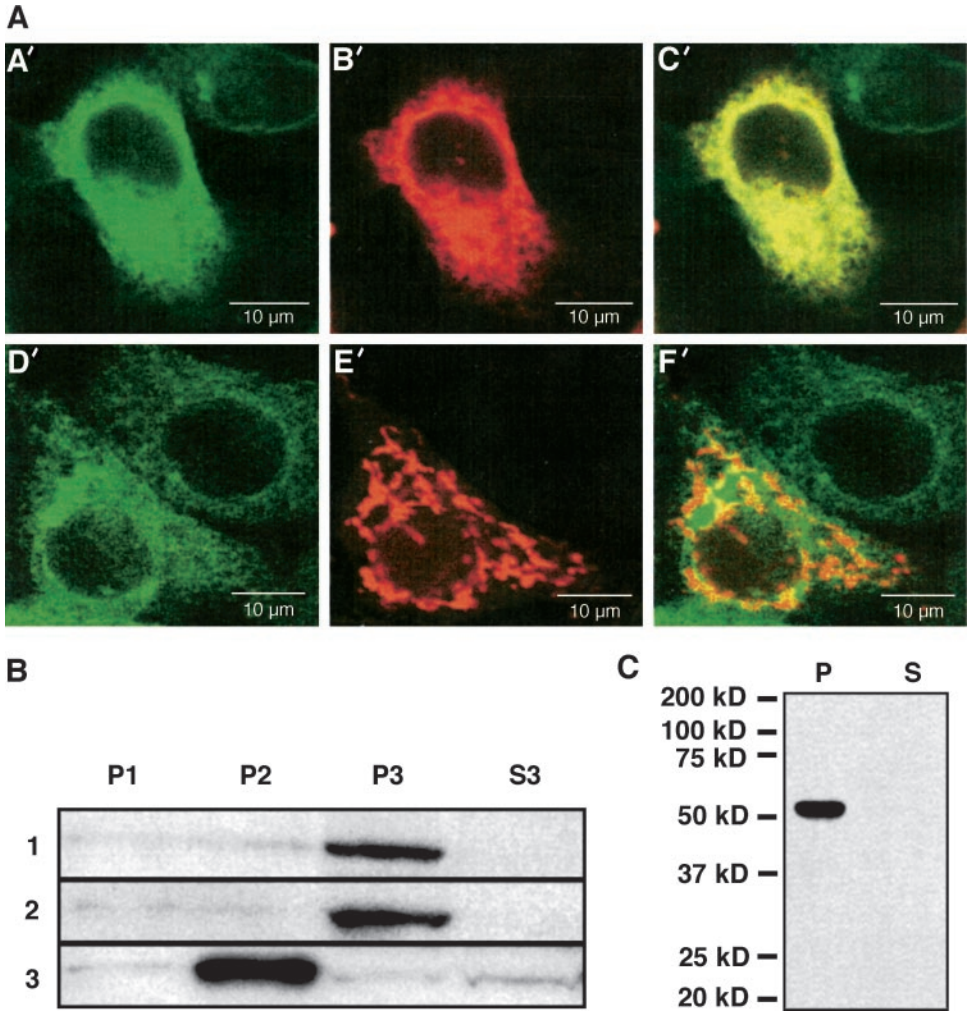

Fig. 6. Subcellular localization of CYP4Z1 in MCF-7 cells. *A*, MCF-7 cells were transiently cotransfected either with vectors pCYP4Z1-EGFP and pmRFP1-endoplasmic reticulum (*A′-C′*) or pCYP4Z1-EGFP and pmRFP1-Mito (*D′-F′*). Twenty-four h after transfection, cells were fixed with paraformaldehyde and examined by confocal laser-scanning microscopy. Representative cells are illustrated. The following expressed fluorescent proteins were detected with filter sets described in "Materials and Methods": CYP4Z1-EGFP (*A′* and *D′*); mRFP1-Sec61 β subunit (*B′*); mRFP1-Mito (*E′*); *C′* and *F′* are superimposed images of *A′* and *B′* or *D′* and *E′*, respectively. *B*, subcellular fractionation of MCF-7 cells transduced with CYP4Z1. Equal volumes of fraction P1 (nuclei and debri), P2 (mitochondria), and P3 (microsomes) and an equivalent volume of S3 (soluble proteins) were subjected to SDS-PAGE and immunoblot analysis for direct comparison of signal intensity. Immunostainings were performed with primary antibodies against CYP4Z1 (1), calnexin (2), or HSP60 (3). *C*, distribution of CYP4Z1 after alkaline sodium carbonate extraction of extrinsic proteins from endoplasmic reticulum membranes. Equivalent volumes of pellet (P) and supernatant (S) after ultracentrifugation were subjected to immunoblot analysis. *EGFP*, enhanced green fluorescent protein; *mRFP1*, monomeric red fluorescent protein 1.

The pseudogene *CYP4Z2P* is localized in head-to-head orientation close to *CYP4Z1* gene on chromosome 1p33. Because of the high-sequence homology of >96% to 4Z1 and its localization on the chromosome, it is likely that *CYP4Z2P* emerged from an inverted duplication event. *CYP4Z2P* cDNA codes for a truncated CYP protein that lacks the sites for substrate binding and for enzymatic activity. *CYP4Z2P* obviously belongs to the class of CYP pseudogenes that are transcriptionally active. However, the transcription level of *CYP4Z2P* is very low in comparison with that of *CYP4Z1*, indicating the expected mRNA degradation of a truncated and presumably nonfunctional CYP.

Quantitative real-time RT-PCR allows thorough investigation of specific gene transcription even in a large gene family like the human CYP family. Comparisons between *CYP* transcription levels and their metabolic activities showed a close relationship for many CYPs, which justifies the prediction of the presence of CYP enzymes based on mRNA levels (40). Our findings demonstrate a highly preferential expression of *CYP4Z1* and *CYP4Z2P* cDNA in breast carcinoma tissue and mammary gland, and verify CYP4Z1 protein expression in breast tissue specimens. Even in liver, known as the organ with the highest accumulation of CYP proteins, expression of CYP4Z1 was 86-fold lower than in breast carcinoma, and CYP4Z2P was not detectable at all. This high expression of CYP4Z1 combined with its specificity to breast tissue is a unique feature among the large CYP family. Studies investigating the expression of a broad range of CYP isoforms approved the existence of CYP 1A1, 1B1, 2A6, 2C, 2B6, 2D6, 2E1, 3A4, 4A11, and 4B1 in different breast tissues including breast cancer (41–44), but revealed an up to 500 times lower expression level in mammary gland than in liver (42), whereas earlier attempts even failed to detect some CYP isoforms in breast microsomes by Western blotting (45). Most of these CYP isoforms have shown the ability to convert xenobiotics into toxins that are carcinogenic in extrahepatic tissues (44). On the other hand, the expression of CYP enzymes in tumor tissues can have a major impact on the responsiveness of tumors to cancer chemotherapeutic drugs, because of the central role that these enzymes play in the metabolism of numerous clinically useful anticancer agents (9, 13). Investigating a broad range of different tumor types confirmed the predominantly breast-restricted expression pattern of CYP4Z1 with a variation of intensity within the breast samples. Furthermore, CYP4Z1 was clearly overexpressed in 52% of breast carcinoma samples in comparison to their corresponding normal tissues. A relatively new approach for cancer treatment is the transfer of *CYP* genes, mainly CYP2B1, 2B6, and 3A4, into cancerous tissue, which confers the capability to activate anticancer prodrugs (*e.g.*, cyclophosphamide or ifosfamide) directly within the target tissue. Preclinical studies have shown dramatically enhanced chemosensitivity of tumors without increased systemic distribution of active drugs by the liver (46, 47). The natural expression of CYP4Z1 in breast cancer tissue might open opportunities for designing future anticancer prodrugs that can specifically be turned into active agents by CYP4Z1 in breast target tissue without the artificial transfer of *CYP* genes into target tissue. However, substrate specificity and enzymatic properties have to be determined to elucidate the physiological function of CYP4Z1 expression in mammary gland and its possible consequences for breast cancer treatment.

In addition to approaches concerning the biochemical and toxicological properties of CYP4Z1, the high association to mammary gland and the overexpression in breast cancer might offer possibilities for immunotherapy based on antigen vaccination and diagnosis of breast cancer. CYP1B1 was found to be overexpressed in various types of tumors but is not expressed in most normal tissues (24) and was consequently classified as a shared tumor-associated antigen (48). Recently, Maecker *et al.* (49) identified HLA-A2-restricted peptides from CYP1B1 that could activate $CD8^+$ T lymphocytes in transgenic mice. Furthermore, they were able to induce CYP1B1-specific T cells by *in vitro*-restimulation from cancer patients that lysed a variety of different CYP1B1-expressing cancer cell lines. Experiments in transgenic mice and preliminary results of a clinical trial did not give any evidence of side effects by autoimmunity.

The data obtained in our study support the potential of CYP4Z1 in this respect and warrant investigations to verify CYP4Z1 as a promising breast cancer antigen.

ACKNOWLEDGMENTS

We would like to thank Lars Kuerschner (Max Planck Institute of Molecular Cell Biology and Genetics, Dresden, Germany) for kindly providing the vectors pmRFP1-ER and pmRFP1-Mito.

REFERENCES

1. American Cancer Society. Cancer facts and figures, 2003. Atlanta, GA: American Cancer Society; 2003. p. 4–9.
2. Scanlan MJ, Jäger D. Challenges to the development of antigen-specific breast cancer vaccines. Breast Cancer Res 2001;3:95–8.
3. Omura T. Forty years of cytochrome P450. Biochem Biophys Res Commun 1999; 266:690–8.
4. Guengerich FP. Common and uncommon cytochrome P450 reactions related to metabolism and chemical toxicity. Chem Res Toxicol 2001;14:611–50.
5. Nelson DR. The cytochrome P450 homepage. http://drnelson.ut-mem.edu/CytochromeP450.html., 2003.
6. Capdevila JH, Falck JR, Harris RC. Cytochrome P450 and arachidonic acid bioactivation: molecular and functional properties of the arachidonate monooxygenase. J Lipid Res 2000;41:163–81.
7. Ortiz de Montellano, PR, Chan, WK, Tuck, SF, Kaikaus, RM, Bass, NM, and Peterson, JA. Mechanism-based probes of the topology and function of fatty acid hydroxylases. FASEB J 1992;6:695–9.
8. Pelkonen O, Raunio H. Metabolic activation of toxins: tissue-specific expression and metabolism in target organs. Environ Health Perspect 1997;105(Suppl 4):767–74.
9. Krishna DR, Klotz U. Extrahepatic metabolism of drugs in humans. Clin Pharmacokinet 1994;26:144–60.
10. Guengerich FP. Metabolism of chemical carcinogens. Carcinogenesis (Lond) 2000; 21:345–51.
11. Murray GI, Taylor MC, McFadyen MCE, et al. Tumor-specific expression of cytochrome P450 CYP1B1. Cancer Res 1997;57:3026–31.
12. Murray GI. The role of cytochrome P450 in tumour development and progression and its potential in therapy. J Pathol 2000;192:419–26.
13. Kivistö KT, Kroemer HK, Eichelbaum M. The role of human cytochrome P450 enzymes in the metabolism of anticancer agents: implications for drug interactions. Br J Clin Pharmacol 1995;40:523–30.
14. Quintieri L, Rosato A, Napoli E, et al. In vivo antitumor activity and host toxicity of methoxymorpholinyl doxorubicin: role of cytochrome P450 3A. Cancer Res 2000; 60:3232–8.
15. Anttila S, Hietanen E, Vainio H, et al. Smoking and peripheral type of cancer are related to high levels of pulmonary cytochrome P450IA in lung cancer patients. Int J Cancer 1991;47:681–5.
16. Massaad L, de Waziers I, Ribrag V, et al. Comparison of mouse and human colon tumors with regard to phase I and phase II drug-metabolizing enzyme systems. Cancer Res 1992;52:6567–75.
17. Toussaint C, Albin N, Massaad L, et al. Main drug- and carcinogen-metabolizing enzyme systems in human non-small cell lung cancer and peritumoral tissues. Cancer Res 1993;53:4608–12.
18. Murray GI, Taylor MC, Burke MD, Melvin WT. Enhanced expression of cytochrome P450 in stomach cancer. Br J Cancer 1998;77:1040–4.
19. McKay JA, Murray GI, Weaver RJ, Ewen SW, Melvin WT, Burke MD. Xenobiotic metabolising enzyme expression in colonic neoplasia. Gut 1993;34:1234–9.
20. Larsen MC, Angus WG, Brake PB, Eltom SE, Sukow KA, Jefcoate CR. Characterization of CYP1B1 and CYP1A1 expression in human mammary epithelial cells: role of the aryl hydrocarbon receptor in polycyclic aromatic hydrocarbon metabolism. Cancer Res 1998;58:2366–74.
21. Wang H, Dick R, Yin H, et al. Structure-function relationships of human liver cytochromes P450 3A: aflatoxin B1 metabolism as a probe. Biochemistry 1998;37: 12536–45.
22. McKinnon RA, Burgess WM, Hall PM, Roberts-Thomson SJ, Gonzalez FJ, McManus ME. Characterisation of CYP3A gene subfamily expression in human gastrointestinal tissues. Gut 1995;36:259–67.
23. Patten CJ, Smith TJ, Murphy SE, et al. Kinetic analysis of the activation of 4-(methylnitrosamino)-1-(3-pyridyl)-1-butanone by heterologously expressed human P450 enzymes and the effect of P450-specific chemical inhibitors on this activation in human liver microsomes. Arch Biochem Biophys 1996;333:127–38.
24. Murray GI, Melvin WT, Greenlee WF, Burke MD. Regulation, function, and tissue-specific expression of cytochrome P450 CYP1B1. Annu Rev Pharmacol Toxicol 2001;41:297–316.

25. Shimada T, Hayes CL, Yamazaki H, et al. Activation of chemically diverse procarcinogens by human cytochrome P-450 1B1. Cancer Res 1996;56:2979–84.
26. Crespi CL, Penman BW, Steimel DT, Smith T, Yang CS, Sutter TR. Development of a human lymphoblastoid cell line constitutively expressing human CYP1B1 cDNA: substrate specificity with model substrates and promutagens. Mutagenesis 1997;12:83–9.
27. Hayes CL, Spink DC, Spink BC, Cao JQ, Walker NJ, Sutter TR. 17β-estradiol hydroxylation catalyzed by human cytochrome P450 1B1. Proc Natl Acad Sci USA 1996;93:9776–81.
28. Cavalieri EL, Stack DE, Devanesan PD, et al. Molecular origin of cancer: catechol estrogen-3,4-quinones as endogenous tumor initiators. Proc Natl Acad Sci USA 1997;94:10937–42.
29. Imaoka S, Yoneda Y, Sugimoto T, et al. CYP4B1 is a possible risk factor for bladder cancer in humans. Biochem Biophys Res Commun 2000;277:776–80.
30. Verschoyle RD, Philpot RM, Wolf CR, Dinsdale D. CYP4B1 activates 4-ipomeanol in rat lung. Toxicol Appl Pharmacol 1993;123:193–8.
31. Imaoka S, Yoneda Y, Matsuda T, Degawa M, Fukushima S, Funae Y. Mutagenic activation of urinary bladder carcinogens by CYP4B1 and the presence of CYP4B1 in bladder mucosa. Biochem Pharmacol 1997;54:677–83.
32. Temme A, Rieger M, Reber F, et al. Localization, dynamics, and function of survivin revealed by expression of functional survivinDsRed fusion proteins in the living cell. Mol Biol Cell 2003;14:78–92.
33. Soneoka Y, Cannon PM, Ramsdale EE, et al. A transient three-plasmid expression system for the production of high titer retroviral vectors. Nucleic Acids Res 1995;23:628–33.
34. Laemmli UK. Cleavage of structural proteins during assembly of the head of bacteriophage T4. Nature (Lond) 1970;396:580–4.
35. Campbell RE, Tour O, Palmer AE, et al. A monomeric red fluorescent protein. Proc Natl Acad Sci USA 2002;99:7877–82.
36. Rolls MM, Stein PA, Taylor SS, Ha E, McKeon F, Rapoport TA. A visual screen of a GFP-fusion library identifies a new type of nuclear envelope membrane protein. J Cell Biol 1999;146:29–44.
37. Ni L, Heard TS, Weiner H. In vivo mitochondrial import. A comparison of leader sequence charge and structural relationships with the in vitro model resulting in evidence for co-translational import. J Biol Chem. 1999;274:12685–91.
38. Clark BJ, Waterman MR. The hydrophobic amino-terminal sequence of bovine 17 α-hydroxylase is required for the expression of a functional hemoprotein in COS 1 cells. J Biol Chem 1991;266:5898–904.
39. Graham-Lorence S, Peterson JA. P450s: structural similarities and functional differences. FASEB J 1996;10:206–14.
40. Rodriguez-Antona C, Donato MT, Pareja E, Gómez-Lechón, M-J, and Castell JV. Chytochrome P-450 mRNA expression in human liver and its relationship with enzyme activity. Arch Biochem Biophys 2001;393:308–15.
41. McKay JA, Melvin WT, Ah-See AK, et al. Expression of cytochrome P450 CYP1B1 in breast cancer. FEBS Lett 1995;374:270–2.
42. Hellmold H, Rylander T, Magnusson M, Reihnér E, Warner M, Gustafsson J-Å. Characterization of cytochrome P450 enzymes in human breast tissue from reduction mammaplasties. J Clin Endocrinol Metab 1998;83:886–95.
43. Spink DC, Spink BC, Cao JQ, et al. Differential expression of CYP1A1 and CYP1B1 in human breast epithelial cells and breast tumor cells. Carcinogenesis (Lond) 1998;19:291–8.
44. Williams JA, Phillips DH. Mammary expression of xenobiotic metabolizing enzymes and their potential role in breast cancer. Cancer Res 2000;60:4667–77.
45. Albin N, Massaad L, Toussaint C, et al. Main drug-metabolizing enzyme systems in human breast tumors and peritumoral tissues. Cancer Res 1993;53:3541–6.
46. Chen L, Waxman DJ, Chen D, Kufe DW. Sensitization of human breast cancer cells to cyclophosphamide and ifosfamide by transfer of a liver cytochrome P450 gene. Cancer Res 1996;56:1331–40.
47. Jounaidi Y, Waxman DJ. Frequent, moderate-dose cyclophosphamide administration improves the efficacy of cytochrome P-450/cytochrome P-450 reductase-based cancer gene therapy. Cancer Res 2001;61:4437–44.
48. Gordan JD, Vonderheide RH. Universal tumor antigens as targets for immunotherapy. Cytotherapy 2002;4:317–27.
49. Maecker B, Sherr DH, Vonderheide RH, et al. The shared tumor-associated antigen cytochrome P450 1B1 is recognized by specific cytotoxic T cells. Blood 2003;102:3287–94.